

## A Three-Dimensional Coordination Polymer Featuring Effective Ferrimagnetic Hydroxide-Bridged Manganese(II) Chains

Jin-Tang Li,<sup>†</sup> Jun Tao,<sup>\*,†</sup> Rong-Bin Huang,<sup>†</sup> Lan-Sun Zheng,<sup>†</sup> Tan Yuen,<sup>‡</sup> C. L. Lin,<sup>‡</sup> Princy Varughese,<sup>§</sup> and Jing Li<sup>\*,§</sup>

Department of Chemistry and State Key Laboratory for Physical Chemistry of Solid Surface, Xiamen University, Xiamen 361005, China, Department of Physics, Temple University, Philadelphia, Pennsylvania 19122, and Department of Chemistry and Chemical Biology, Rutgers University, 610 Taylor Road, Piscataway, New Jersey 08854

Received January 12, 2005

A three-dimensional coordination polymer,  $[\text{Mn}_3(\text{OH})_2\text{Na}_2(3\text{-cnba})_6]_n$  (**1**) (3-Hcnba = 3-cyanobenzoic acid), has been synthesized by the reaction of  $\text{MnCl}_2$ ,  $\text{NaN}_3$ , and 3-Hcnba in water. Its crystal structure was determined by single-crystal X-ray diffraction. Magnetic studies show that the complex behaves as a three-dimensional metamagnet built from effective ferrimagnetic Mn(II) chains in which spin moments are linked by interactions in an AF–F–AF (F = ferromagnetic and AF = antiferromagnetic) sequence in the triangular magnetic repeating unit.

Coordination polymers exhibiting magnetic properties are of great interest in the field of molecular magnetism and materials chemistry.<sup>1</sup> The exchange coupling among homometallic paramagnetic centers in these materials typically leads to ferromagnetic<sup>2</sup> or antiferromagnetic<sup>3</sup> behavior, whereas ferrimagnetism, a phenomenon often observed in heterometallic systems in which two different kinds of magnetic centers alternate regularly and interact antiferromagnetically, has been relatively less investigated in homo-

metallic coordination polymers.<sup>4</sup> This is mainly due to the fact that ferrimagnetic conditions for the noncompensation in spin moments are difficult to achieve in this type of structure. Recent studies indicate that homometallic ferrimagnetic compounds must have molecular topology with a specific alternation of ferro- and antiferromagnetic interactions, such as those containing homometallic odd-sided polyhedral coupling units.<sup>4,5</sup> In homometallic triangular topologic structures (the simplest odd-sided polyhedra), it is relatively easy to achieve such coupling, and such structures can, therefore, be a useful prototype for attaining homometallic ferrimagnetism. Here, we report a three-dimensional metamagnetic coordination polymer,  $[\text{Mn}_3(\text{OH})_2\text{Na}_2(\text{C}_8\text{H}_4\text{NO}_2)_6]_n$  (**1**), containing effective ferrimagnetic Mn(II) chains built from  $\mu_3$ -hydroxide-bridged triangular Mn(II) repeating units.

Colorless needle crystals of **1** were obtained by slow evaporation of an aqueous solution containing  $\text{MnCl}_2 \cdot 4\text{H}_2\text{O}$ , 3-Hcnba, and  $\text{NaN}_3$  in a molecular ratio of 1:2:2 at room temperature.<sup>6</sup>  $\text{N}_3^-$  is not involved in coordination to man-

\* To whom correspondence should be addressed. E-mail: taojun@jingxian.xmu.edu.cn (J.T.), jingli@rutchem.rutgers.edu (J.L.).

<sup>†</sup> Xiamen University.

<sup>‡</sup> Temple University.

<sup>§</sup> Rutgers University.

- (1) (a) Kahn, O. *Molecular Magnetism*; VCH: Weinheim, Germany, 1993. (b) *Magnetism: Molecules to Materials II: Molecule-Based Materials*; Miller, J. S., Drillon, M., Eds.; Wiley-VCH: Weinheim, Germany, 2002. (c) Cernak, J.; Orendac, M.; Potocnak, I.; Chomic, J.; Orendacova, A.; Skorsepa, J.; Feher, A. *Coord. Chem. Rev.* **2002**, *224*, 51. (2) (a) Tang, L. F.; Zhang, L.; Li, L. C.; Cheng, P.; Wang, Z. H.; Wang, J. T. *Inorg. Chem.* **1999**, *38*, 6326. (b) Li, L. C.; Liao, D. Z.; Jiang, Z. H.; Yan, S. P. *Inorg. Chem.* **2002**, *41*, 1019. (c) Bu, X. H.; Liu, H.; Du, M.; Zhang, L.; Guo, Y. M.; Shionoya, M.; Ribas, J. *Inorg. Chem.* **2002**, *41*, 1855. (d) Kumagai, H.; Ohba, M.; Inoue, K.; Okawa, H. *Chem. Lett.* **2002**, 1006. (e) Liu, T. F.; Sun, H. L.; Gao, S.; Zhang, S. W.; Lau, T. C. *Inorg. Chem.* **2003**, *42*, 4792. (3) (a) Kim, Y.; Jung, D. P. *Inorg. Chem.* **2000**, *39*, 1470. (b) Mukherjee, P. S.; Maji, T. K.; Mostafa, G.; Hibbs, W.; Chaudhuri, N. R. *New J. Chem.* **2001**, *25*, 760. (c) Lee, E.; Kim, Y.; Jung, D. Y. *Inorg. Chem.* **2002**, *41*, 501. (d) Papaefstathiou, G. S.; Vicente, R.; Raptopoulou, C. P.; Terzis, A.; Escuer, A.; Perlepes, S. P. *Eur. J. Inorg. Chem.* **2002**, 2488. (e) Li, Y. G.; Hao, N.; Wang, E. B.; Lu, Y.; Hu, C. W.; Xu, L. *Eur. J. Inorg. Chem.* **2003**, 2567.

- (4) (a) Chen, H. J.; Mao, Z. W.; Gao, S.; Chen, X. M. *Chem. Commun.* **2001**, 2320. (b) Guillou, N.; Pastre, S.; Livage, C.; Ferey, G. *Chem. Commun.* **2002**, 2358. (c) Konar, S.; Mukherjee, P. S.; Zangrando, E.; Lloret, F.; Chaudhuri, N. *Angew. Chem., Int. Ed.* **2002**, *41*, 1561. (d) Wang, R. H.; Gao, E. Q.; Hong, M. C.; Gao, S.; Luo, J. H.; Lin, Z. Z.; Han, L.; Cao, R. *Inorg. Chem.* **2003**, *42*, 5486. (e) Wang, Z. M.; Zhang, B.; Fujiwara, H.; Kobayashi, H.; Kurmoo, M. *Chem. Commun.* **2004**, 416. (5) (a) Tong, M. L.; Kitagawa, S.; Chang, H. C.; Ohba, M. *Chem. Commun.* **2004**, 418. (b) Gao, E. Q.; Yue, Y. F.; Bai, S. Q.; He, Z.; Yan, C. H. *J. Am. Chem. Soc.* **2004**, *126*, 1419. (c) Salah, M. B.; Vilminot, S.; Andre, G.; Richard-Plouet, M.; Bouree-Vigneron, F.; Mhiri, T.; Kurmoo, M. *Chem. Eur. J.* **2004**, *10*, 2048. (6) Preparation of **1**:  $\text{MnCl}_2 \cdot 4\text{H}_2\text{O}$  (1.0 mmol),  $\text{NaN}_3$  (2.0 mmol), and 3-cyanobenzoic acid (2.0 mmol) were dissolved in water (10 mL) and stirred for 15 min at 50 °C. In 3 weeks, the filtrate was filtered 2–3 times to remove gray powder. Colorless single crystals were collected from the filtrate in 4 weeks (yield: 0.145 g, ~40% based on manganese), and they rapidly turned to gray in air. Anal. Calcd for  $\text{C}_{48}\text{H}_{26}\text{Mn}_3\text{N}_6\text{Na}_2\text{O}_{14}$  (%): C, 51.40, H, 2.34, N, 7.49. Found: C, 52.00, H, 2.46, N, 7.15. IR (KBr,  $\text{cm}^{-1}$ ): 3617 (w), 3435 (m, br), 3070 (w), 2241 (m), 2103 (m), 1608 (s), 1565 (s), 1432 (s), 1398 (vs), 1206 (w), 1086 (w), 912 (w), 767 (m), 702 (m), 670 (m), 567 (w), 524 (w), 411 (w).

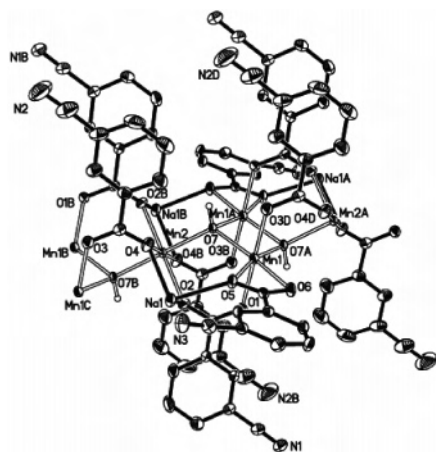
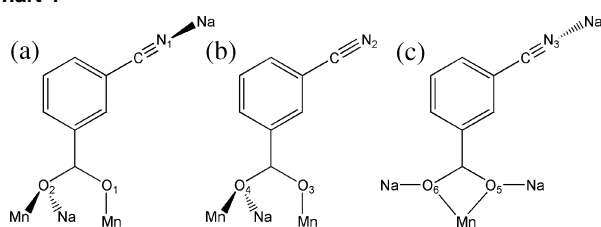


**Figure 1.** ORTEP drawing (35% thermal ellipsoids) showing the metal coordination environment of **1** with atomic numberings. For clarity, the coordination geometry of sodium ions is only drawn partially.

#### Chart 1



ganese(II) or sodium(I) ions, but is essential to act as a base to deprotonate 3-Hcnba. A similar reaction using NaOH as the base produced unidentified powder but not **1**.

X-ray diffraction analysis<sup>7</sup> indicates that the asymmetric unit of **1** contains two crystallographically independent Mn(II) ions and one Na(I) ion (Figure 1). Mn1 and Mn1A ( $-x + 1, -y, -z$ ) are doubly bridged by  $\mu_3$ -hydroxide moieties (O7 and O7A) with a Mn1...Mn1A distance of 3.203 Å. Mn2 is located at a center of symmetry (*i*) and is connected to two Mn1 via two  $\mu_3$ -hydroxide groups. The Mn1–Mn2 and Mn1A–Mn2 distances are 3.683 and 3.710 Å, respectively, thus forming a chain of hydroxide-bridged scalene triangles that share edges and vertices: Mn1 and Mn1A form the shared edge, and Mn2 is at the shared vertex. Mn1 and Mn2 are both octahedrally coordinated, and their coordination spheres are completed by ligand carboxylate-*O* moieties, with an average Mn1–carboxylate-*O* distance 0.06 Å longer than the Mn2–carboxylate-*O* distance. It is noteworthy that the O–Mn2–O trans angles are 180.0° and the O–Mn2–O cis angles lie in the range from 86.6(1) to 93.5(1)°, with a deviation of  $\pm 3.5^\circ$  from the ideal 90° value required for a purely octahedral coordination geometry. Na1 resides in a highly distorted octahedral geometry and is coordinated by four  $\eta^2$ -carboxylate-*O* moieties and two cyano nitrogen atoms. The 3-cnba ligands in **1** have three distinctly different coordination modes in bridging metal ions: One acts as a tetradentate bridge through its cyano nitrogen atom and

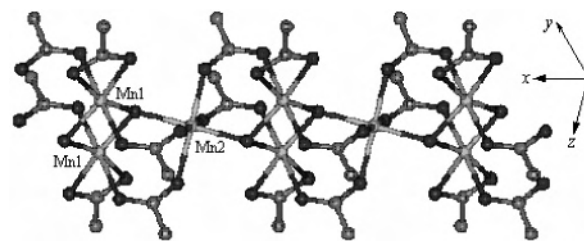


**Figure 2.** Diagram showing the distinct linked Mn atoms; cyanobenzene groups were omitted for clarity.

carboxylate group; the cyano nitrogen atom is coordinated to one Na(I) ion in an adjacent chain, and the carboxylate group forms tridentate bonds through its two oxygen atoms, coordinating to two Mn(II) ions in a syn–syn mode and to one Na(I) ion with the  $\eta^2$ -oxygen (Chart 1a). The second forms a  $\mu^3, \eta^1, \eta^2$ -carboxylate bridge, binding two Mn(II) ions in a syn–syn mode and one Na(I) with the  $\eta^2$ -oxygen (Chart 1b). The carboxylate group of Chart 1b is hardly differentiated from that of Chart 1a with respect to the Mn–O or Na–O distances, but can only be distinguished from the  $\eta^2$ -oxygen binding angles [Mn–O2–Na = 97.2(1)°, Mn–O4–Na = 99.7(1)°]. The third adopts a pentadentate bridging mode, with the cyano nitrogen atom coordinating to one Na(I) ion in an adjacent chain and the carboxylate group chelating one Mn(II) ion and coordinating to two Na(I) ions with the two  $\eta^2$ -oxygen in an anti–anti mode (Chart 1c).

Each  $[\text{Mn}_3(\text{OH})_2\text{Na}_2]_n^{6n+}$  chain is capped by carboxylate groups of 3-cnba ligand and linked to four adjacent ones via the Na–cyano-*N* interactions, thus resulting in a three-dimensional coordination polymer with one-dimensional channels occupied by free cyanobenzene moieties (Chart 1b); the hydroxide-linked Mn(II) atoms are propagated along the *a* axis, and the shortest Mn–Mn interchain distances are 13.194 Å along the *b* axis and 11.232 Å along the *c* axis (Figure 2).

Isothermal magnetization,  $M(H)$ , and magnetic susceptibility, defined as  $\chi(T) = M(T)/H$ , with  $T$  ranging from 1.9 to 300 K and  $H$  up to 54 kG were measured on powder samples of **1**, using a SQUID magnetometer. The results of  $\chi(T)$  measured under applied fields of  $H \geq 100$  G did not show any obvious anomaly except for a large enhancement at low temperatures. However, careful measurements at small  $H$  revealed an antiferromagnetic ground state for this compound. Shown in Figure 3 are the  $\chi(T)$  values measured under several applied fields. Clear cusp-like anomalies indicating an antiferromagnetic phase transition are seen in the data curves for  $H \leq 40$  G.

$\chi(T) \cdot T$  vs  $T$  and  $1/\chi(T)$  vs  $T$  measured with a field of 500 G are plotted in Figure 4 and its inset. For temperatures above 100 K,  $\chi(T)$  can be fitted to a Curie–Weiss law with  $\theta = -78.0$  K and an effective moment of  $\mu_{\text{eff}} = 5.88 \mu_{\text{B}}$ , close to what is expected for a free  $\text{Mn}^{2+}$  ion. In the high- $T$  region,  $\chi \cdot T$  decreases as  $T$  decreases, indicating an overall antiferromagnetic coupling among the  $\text{Mn}^{2+}$  ions. As  $T$  is further lowered,  $\chi \cdot T$  reaches a minimum at around 30 K and then increases rapidly to a maximum at 3 K.

The values of isothermal magnetization,  $M(H)$ , measured at 1.9 K are shown in Figure 5. Isothermal magnetization

(7) Crystal data for **1**:  $\text{C}_{48}\text{H}_{26}\text{Mn}_3\text{N}_6\text{Na}_2\text{O}_{14}$ ,  $M = 1121.55$ , triclinic,  $P\bar{1}$ ,  $a = 6.6633(5)$  Å,  $b = 12.9710(11)$  Å,  $c = 14.1613(12)$  Å,  $\alpha = 70.127(1)^\circ$ ,  $\beta = 88.428(1)^\circ$ ,  $\gamma = 76.473(1)^\circ$ ,  $V = 1117.3(2)$  Å<sup>3</sup>,  $Z = 1$ ,  $D_c = 1.667$  Mg m<sup>-3</sup>,  $R1 = 0.0679$ ,  $wR2 = 0.1653$ ,  $T = 296(2)$  K,  $\mu = 0.934$  mm<sup>-1</sup>,  $S = 1.081$ .

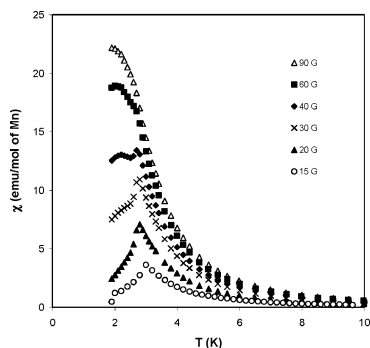


**Figure 3.**  $\chi(T)$  measured at several applied fields of  $H = 15, 20, 30, 40, 60,$  and  $90$  G.

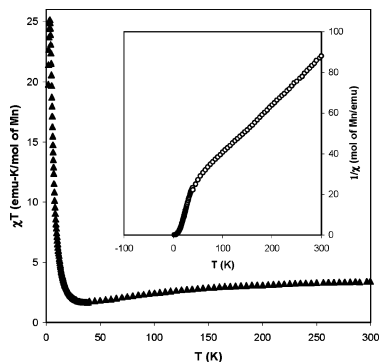


**Figure 4.**  $\chi(T) \cdot T$  vs  $T$  and  $1/\chi(T)$  vs  $T$  (inset) measured at an applied field of  $H = 500$  G.

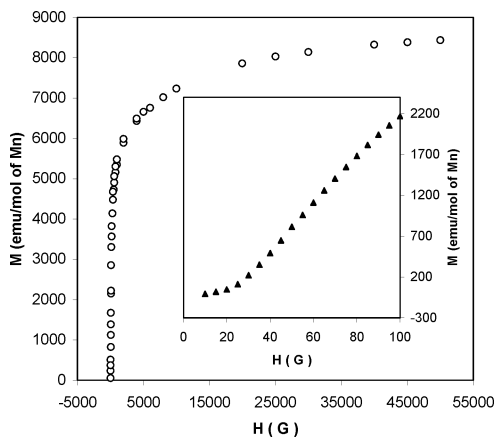


**Figure 5.**  $M(H)$  vs  $H$  measured at  $1.9$  K. The inset is a plot of the data in the low-field region from a measurement with small steps.

experiments were performed, and no sizable hysteresis was observed. As seen in the inset, a sudden change in the slope of  $M(H)$  is observed at a very small critical field of  $H_c \approx 20$  G, suggesting a metamagnetic transition. This is consistent with the  $\chi(T)$  results discussed above. The features exhibited in the  $M(H)$  vs  $H$  data in the region of  $H \geq H_c$  very much resemble those for a ferromagnet or a ferrimagnet in the

ordered state: As  $H$  increases,  $M(H)$  increases rapidly and becomes somewhat saturated above  $10$  kG. At  $H = 50$  kG,  $M(H)$  reaches a value of  $8430$  emu·G/mol of Mn. This value is equivalent to  $1.7 \mu_B$  per  $\text{Mn}^{2+}$  ion, which is very close to one-third of the saturation moment of a free  $\text{Mn}^{2+}$  ion ( $5.9 \mu_B$ ). We can therefore interpret that the metamagnetic transition leads the system to an field-induced ordered state in which two-thirds of the  $\text{Mn}^{2+}$  moments are oriented in one direction and the other one-third are oriented in an opposite direction.

The complexity of the magnetic behavior presented in **1** originates from the special magnetic couplings of the  $\text{Mn}^{2+}$  ions in the chains, where alternating  $\text{Mn}^{2+}$ – $\text{Mn}^{2+}$  dimer units and  $\text{Mn}^{2+}$  single ion units are connected along the  $a$  axis. Suitable theoretical models are needed to describe the low- $T$  region of the  $\chi(T)$  data. By considering the symmetry at the  $\text{Mn}^{2+}$  sites and comparing to other similar compounds involving hydroxide-bridged Mn(II) networks such as in ref 5c, it can be speculated that the exchange interaction between the two  $\text{Mn}^{2+}$  ions in the dimer is dominantly positive (ferromagnetic) and the interaction between the single  $\text{Mn}^{2+}$  ion and the  $\text{Mn}^{2+}$  ions in the dimer is dominantly negative (antiferromagnetic). Such intrachain magnetic interactions would effectively produce ferrimagnetic chains in the system. However, because of the noncollinear orientations of the octahedral  $\text{Mn}^{2+}$  centers at their different sites, it is most likely that the spin orientations of the  $\text{Mn}^{2+}$  ions at different sites are also noncollinear. There seem to be antiferromagnetic interchain interactions between the effective ferrimagnetic chains so that a 3D antiferromagnetic ground state, rather than a simple spontaneous ferrimagnetic ordered state, is achieved at sufficient low  $T$ . Yet, from the fact that  $H_c$  is so small, one might expect that the antiferromagnetic interchain coupling is very weak. Further studies on the details of the Mn–Mn coupling within the ( $\text{Mn}^{2+}$  dimer)– $\text{Mn}^{2+}$ –( $\text{Mn}^{2+}$  dimer) chains and the interaction among these chains are needed to obtain a full picture of the magnetic behavior in this system.

**Acknowledgment.** This work was financially supported by the National Natural Science Foundation of China (20301014) and the Innovation Foundation for Young Scientific Talents of Fujian Province of China (2002J004). P.V. and J.L. acknowledge partial support from the National Science Foundation via DMR-0422932. T.Y. and C.L. acknowledge GIA support from Temple University.

**Supporting Information Available:** X-ray data in CIF file are available free of charge via the Internet at <http://pubs.acs.org>.

IC050043M